

Polymorphs and Solvates of a Cocrystal Involving an Analgesic Drug, Ethenzamide, and 3,5-Dinitrobenzoic Acid

Srinivasulu Aitipamula,^{*,†} Pui Shan Chow,[†] and Reginald B. H. Tan^{*,†,‡}

[†]Crystallization and Particle Science, Institute of Chemical and Engineering Sciences, A*STAR (Agency for Science, Technology and Research), 1, Pesek Road, Jurong Island, Singapore, 627833, and

[‡]Department of Chemical & Biomolecular Engineering, National University of Singapore 4, Engineering Drive 4, Singapore 117576

Received December 4, 2009; Revised Manuscript Received March 14, 2010

ABSTRACT: A 1:1 cocrystal involving an analgesic drug, ethenzamide (EA), and 3,5-dinitrobenzoic acid exists in two polymorphs and forms a series of solvates. All the crystalline materials have been characterized by various analytical techniques, such as single-crystal and powder X-ray diffraction, ¹H NMR, and DSC/TGA. It was found that one of the polymorphs (form II) and the solvates, except mesitylene solvate, contain a common hydrogen-bonded tetrameric motif in their crystal structures. Desolvation of all the solvates resulted in form I and the process features the switch over of supramolecular synthon from amide–amide homosynthon to an acid–amide heterosynthon. This observation was rationalized on the basis of facile transformation of form II into form I at ambient conditions and the structural similarity of form II with that of the structures of solvates. The ability of EA cocrystals to form polymorphs and solvates is compared with statistics extracted from the Cambridge Structural Database on the prevalence of polymorphs and solvates/hydrates in the cocrystals. It was found that the number of polymorphic cocrystals being added to the database is increasing, and the tendency of solvate/hydrate formation is significantly higher for cocrystals when compared to the crystalline solvates/hydrates of a single solid component.

Introduction

Pharmaceutical cocrystallization has emerged as an effective approach to produce a new class of active pharmaceutical ingredients (APIs), which are called pharmaceutical cocrystals, with great potential advantages, alongside polymorphs, salts, solvates/hydrates, and amorphous materials.^{1–4} Pharmaceutical cocrystals are defined as molecular complexes comprised an API and one or more pharmaceutically acceptable cocrystal formers (FDA-approved generally regarded as safe (GRAS) compounds⁵), which are solids at room temperature.⁶ Over the past few years, this new branch of materials has remarkably impacted the field of pharmaceutical research by broadening the intrinsic values of APIs in terms of potential expansion of intellectual property,⁷ as well as enhancement of physicochemical properties, e.g., solubility, dissolution profile, and stability.^{8–14}

Polymorphism is defined as the ability of a substance to exist as two or more crystalline forms.¹⁵ Incorporation of solvent molecules into the crystal lattice produces new solid materials that are variously termed as host–guest complexes, pseudopolymorphs, solvates, and clathrates.^{16–18} The phenomena of polymorphism and guest inclusion have significant importance in pharmaceutical drug development because the resulting solid materials possess unique properties and thus has a huge commercial impact at all stages of API development.¹⁹ Therefore, identification of conditions under which polymorphs/solvates are formed, and characterization of all the possible polymorphs and the products resulting in a desolvation process are of fundamental importance to pharmaceutical industry. Polymorphism is a well-known and probably one of the most widely studied phenomenon in single-component crystals and

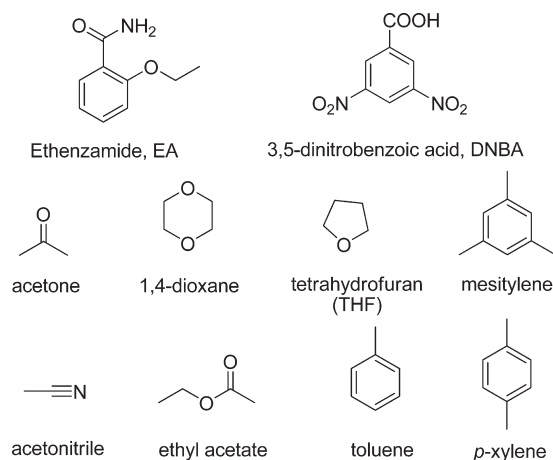
APIs.¹⁵ In the case of cocrystals, studies concerning polymorphism are relatively rare.^{20–27} Though, it has been recently argued that cocrystals are less prone to polymorphism,²⁸ our recent results,^{20,21} as well as some recent studies directed toward finding cocrystal polymorphs^{25,27} have implied that cocrystals can also exist in polymorphic forms. On the other hand, the ability of multicomponent crystals to act as host frameworks has been exemplified, and several heteromolecular lattice hosts have been reported recently.^{29–34}

Ethenzamide (2-ethoxybenzamide, EA) is a nonsteroidal anti-inflammatory drug used mainly in combination with other ingredients, such as acetaminophen, aspirin, dipyron, allyl-isopropylacetylurea, caffeine, and ibuprofen for the treatment of mild to moderate pain.^{35–37} A combination of acetaminophen and EA is the most commonly used analgesic in Japan.³⁸ The crystal structure of EA has been recently solved using high-resolution powder X-ray diffraction.³⁹ We have recently reported two polymorphic cocrystals of EA with saccharin²⁰ and with another API, gentisic acid.²¹ With our interest in exploring the solid form diversity of EA cocrystals, herein we report a 1:1 model cocrystal involving EA and 3,5-dinitrobenzoic acid (DNBA), which can form polymorphs as well as include various guest molecules in the nano channels (see Scheme 1). The cocrystal polymorphs and solvates were characterized by single-crystal X-ray diffraction, DSC/TGA, and ¹H NMR. The propensity of cocrystals to form polymorphs and solvates/hydrates was compared with the polymorphic single-component crystals and crystalline solvates/hydrates in which there is only one solid component by analyzing the crystal structures deposited in the Cambridge Structural Database (CSD).⁴⁰

Experimental Section

Preparation of Cocrystals by Solution Crystallization. EA and DNBA were purchased from Alfa Aesar, and used as received

*E-mail: srinivasulu_aitipamula@ices.a-star.edu.sg (S.A.); reginald_tan@ices.a-star.edu.sg (R.B.H.T.). Tel: (65) 6796 3858. Fax: (65) 6316 6183.

Scheme 1. Molecular Structures of EA, DNBA, and the Solvents That Produced Solvates Reported in This Paper

without any further purification. Analytical grade solvents were used. Crystallization experiments were conducted by dissolving a 1:1 stoichiometric mixture of EA (100 mg, 0.605 mmol) and DNBA (128.3 mg, 0.650 mmol) in a minimum amount of solvent (approximately 3–5 mL) followed by slow evaporation of the solvent at ambient conditions. Whereas form I of the EA·DNBA cocrystal can be easily obtained from common organic solvents, form II was obtained only along with form I crystals from methanol and geraniol (3:1). All the solvates were obtained by slow evaporation of the 1:1 EA and DNBA solution from the respective solvents.

Grinding Experiments. Grinding was performed using a Retsch Mixer Mill model MM301 with 10 mL stainless steel grinding jars with one 7 mm stainless steel grinding ball at a rate of 20 Hz for 15 min. Experiments were carried out with 1:1 stoichiometric ratio of EA and DNBA. Solvent-drop grinding (SDG) experiments were performed by adding ca. 0.05 mL (2 drops from a pipet) of a selected solvent to the reactants prior to the grinding. Water, acetone, ethyl acetate, acetonitrile, ethanol, methanol, 2-propanol, diethyl ether, 1,4-dioxane, toluene, *n*-hexane, cyclohexane, dichloromethane (DCM), and chloroform were used for the SDG experiments. The resulting powder samples were analyzed by PXRD for the cocrystal formation. The external temperature of the grinding jar after completion of the experiments did not exceed ca. 30 °C.

Single-Crystal X-ray Diffraction. X-ray reflections were collected on a Rigaku Saturn CCD area detector with graphite monochromated Mo-K α radiation ($\lambda = 0.71073$ Å). Data were collected and processed using CrystalClear (Rigaku) software. Structures were solved by direct methods and SHELX-TL⁴¹ was used for structure solution and least-squares refinement. The non-hydrogen atoms were refined anisotropically. All hydrogen atoms were fixed at idealized positions except for the N–H, O–H hydrogen atoms which were located from the difference Fourier map and allowed to ride on their parent atoms in the refinement cycles. All O–H, N–H, and C–H distances are neutron normalized to 0.983, 1.009, and 1.083 Å, respectively. X-Seal was used to prepare the figures and packing diagrams. Data collection and refinement details (Table S1), and pertinent hydrogen bond distances (Table S2) were provided in the Supporting Information. Crystal data have been deposited at the Cambridge Crystallographic Data Centre (CCDC) with the deposition numbers: CCDC 752467, 752468, 752470–752472, and 752474–752478. These data can be obtained free of charge via www.ccdc.cam.ac.uk or from the CCDC, 12 Union Road, Cambridge CB21EZ, UK; e-mail: deposit@ccdc.cam.ac.uk.

Powder X-ray Diffraction (PXRD). Powder diffractograms were recorded on a Bruker D8 Advance (Bruker AXS GmbH, Karlsruhe, Germany) in Bragg–Brentano geometry equipped with a Cu-K α source ($\lambda = 1.54056$ Å), 2.5° primary and secondary soler slits, 0.3° divergence slit, an 0.3° antiscatter slit and a position sensitive microgap detector, Vantec-1, (Bruker AXS GmbH, Karlsruhe, Germany). The voltage and current applied were 35 kV and 40 mA, respectively. Samples were placed on a sample holder which has 1 mm thickness and 1.5 cm diameter. The data were collected

over an angle range of 2 to 50° with a scanning speed of 2° per minute.

Differential Scanning Calorimetry (DSC). DSC was performed with a Perkin-Elmer, Diamond DSC with an autosampler. Crystals taken from the mother liquor were blotted dry on a filter paper and manually ground to obtain a fine powder. As confirmed by the PXRD analysis, no form conversion occurred during grinding. The powder was placed in crimped aluminum sample pans. The sample size was 2–5 mg and the heating rate was 5 °C min⁻¹. The samples were purged with a stream of flowing nitrogen (20 mL min⁻¹).

Thermogravimetric Analysis (TGA). TGA was performed on a TA Instruments, TGA Q500 thermogravimetric analyzer. Approximately 15 mg of the sample was added to an alumina crucible. The samples were heated at a constant heating rate of 5 °C min⁻¹. The samples were purged with a stream of flowing nitrogen throughout the experiment at 40 mL min⁻¹.

Microscopic Observations. The crystallization of forms I and II of EA·DNBA cocrystal was visualized with an optical polarizing microscope (Olympus, BX51) equipped with a Linkam hot-stage THMS 600 connected to a TMS 94 temperature controller and a LNP 94/2 liquid nitrogen pump (Linkam Scientific Instruments Ltd., Tadworth, Surrey, UK). The temperature was kept constant at 25 °C. The microscopic images were recorded with a CCD camera attached to the Olympus BX-51 microscope (Olympus Optical GmbH, Vienna, A) at every 10 s time intervals using Soft Imaging System's Analysis image capture software.

Nuclear Magnetic Resonance (NMR) Spectroscopy. All the ¹H NMR spectra were recorded at 400 MHz on a Bruker instrument in DMSO-*d*₆ at 25 °C.

Cambridge Structural Database (CSD). Polymorphs and solvates/hydrates of cocrystals, single component polymorphs and solvates/hydrates were retrieved from the CSD (May 2009 update).⁴⁰ A compound that is liquid at room temperature was considered as a solvent. For all the searches, only the structures with 3D coordinates determined and “no errors”, “no polymeric”, and “no ions” were considered. Structures containing transition elements, actinide, lanthanide, Al, Ga, In, Tl, Ge, Sn, Pb, Sb, Bi, or Po were excluded from the search. All polymorphic structures in which there are two or more chemical units were retrieved with ‘polymorph’ as a keyword. Polymorphic cocrystals were manually separated from the polymorphic solvates/hydrates of a single solid component. Duplicate refcodes were manually removed and only one refcode was counted for each polymorphic set. A table listing all the polymorphic cocrystal sets was provided in the Supporting Information (Table S3). Hydrates were retrieved by searching for the keyword ‘hydrate’ as well as the structure H–O–H. Solvates were identified by searching for the keywords “solvate” or “clathrate”. All these hit lists were manually screened to separate the cocrystal hydrates/solvates from the hydrate/solvates in which there is only one solid component. The parameter “number of chemical units equals to 2” was used to retrieve the hydrates/solvates of single solids, whereas a search for structures containing number of chemical units more than 2 resulted cocrystal hydrate/solvates and multi-solvates or solvate hydrates of single solids. Ternary and quaternary cocrystals were included in total cocrystal structures. A search for pharmaceutical cocrystals which contain at least one API and one or more pharmaceutically acceptable cocrystal formers resulted in 137 (3.8 %) cocrystals of the total 3624 cocrystals.⁴² A list of CSD refcodes found in the CSD analysis was provided in the Supporting Information.

Results and Discussion

Crystallization of EA and DNBA in 1:1 stoichiometric ratio from a 3:1 mixture of methanol and geraniol resulted crystals of two different shapes (block and needle), which belong to different polymorphs. One of the polymorphs (form I, block shape) was also obtained in pure form from a methanol solution; however, attempts to produce form II from common organic solvents were not successful. Crystals of form II are unstable when placed in an open environment at RT and readily transform to the stable form I. Cocrystallization

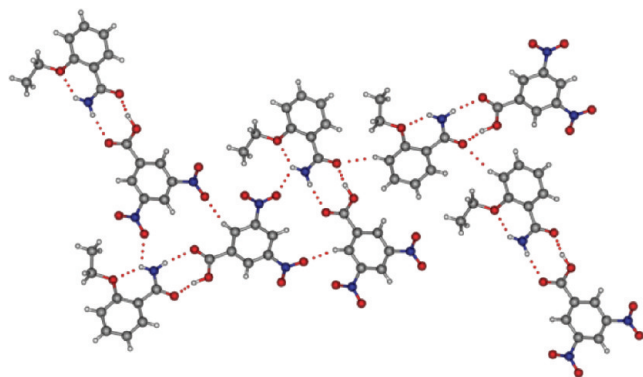


Figure 1. Acid–amide heterosynthon and the herringbone arrangement of dimeric motifs in the crystal structure of form I of EA·DNBA cocrystal.

experiments to produce pure polymorphs of the cocrystal resulted in various solvates. All the solvates are unstable at RT and tend to desolvate when exposed to open air.

Polymorphs. Single-crystal X-ray analysis of a form I crystal confers $P2_1/c$ space group (Table S1, Supporting Information). The *anti*-N–H of the primary amide of EA forms an intramolecular N–H···O (1.9 Å, 130°, see Table S2 in the Supporting Information) hydrogen bond. As shown in Figure 1, a notable interaction that holds EA and DNBA molecules is a heterosynthon between the carboxamide group of EA and acid group of DNBA via N–H···O (2.0 Å, 168°) and O–H···O (1.56 Å, 165°) hydrogen bonds. The dimeric units thus generated were arranged in a herringbone fashion to form zigzag chains along the crystallographic *c*-axis via N–H···O (2.5 Å, 106°) hydrogen bond involving *anti*-N–H of the EA and nitro group of the DNBA (Figure 1). The adjacent zigzag chains are further interconnected via C–H···O (2.39–2.57 Å, 119–157°) interactions. The overall crystal packing also features $\pi\cdots\pi$ stacking interactions between the aromatic rings.

Because form II crystals are unstable at RT, a suitable crystal removed from the solvent was immediately mounted on the diffractometer and purged with a stream of liquid nitrogen. The crystal data confirms it to be a 1:1 cocrystal between EA and DNBA and it belongs to triclinic, $P\bar{1}$ space group. Interestingly, the supramolecular acid–amide heterosynthon observed in form I was absent in form II. Instead the crystal structure reveals a supramolecular amide–amide homosynthon between two inversion related EA molecules. Two DNBA molecules involved in N–H···O (2.41 Å, 109°) and O–H···O (1.63 Å, 168°) hydrogen bonds with EA molecules and connected to either side of the amide–amide homosynthon (Figure 2a). The resulting tetrameric motifs are stabilized in the crystal lattice by several C–H···O (2.43–2.62 Å, 130–172°) and $\pi\cdots\pi$ stacking interactions (Figure 2b).

The fact that EA·DNBA cocrystal forms a series of solvates (discussed in the next section), and form II crystals are unstable when they are removed from the solvent, prompted us to investigate whether form II is a true polymorph or an unstable solvate. A PLATON⁴³ analysis on both the crystal structures reveals that they do not possess solvent accessible voids in the crystal lattice, and thus form II is likely to be a true polymorph. The solvent mediated phase transformation²⁷ from form II to form I was visualized under hot-stage microscopy. A concentrated solution of EA and DNBA in methanol and geraniol (3:1) was kept at a constant

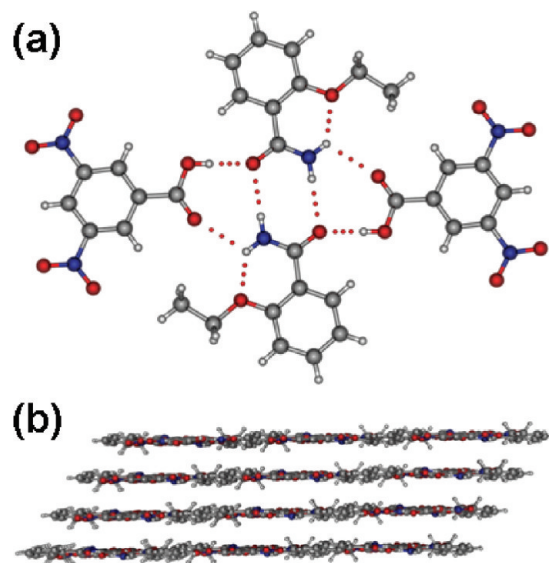


Figure 2. (a) Hydrogen-bonded tetrameric motif in the crystal structure of form II of EA·DNBA cocrystal, which features an amide–amide homosynthon. (b) Stacking of tetrameric motifs.

temperature of 25 °C and allowed to crystallize. Figure 3 shows snapshots of the crystallization event taken at different time intervals. Nucleation and growth of needle-shaped crystals of form II was observed after 10 min. As the crystallization proceeds, crystals of both the polymorphs (form I & II) appeared together and after 1 h there were no crystals of form II and only the block-shaped crystals of form I remained in the solution. This suggests that the metastable form II forms first which then converts to the stable form I. form I being the stable Form is also confirmed by lattice energy calculations (form I, −52.39, form II, −46.29 kcal mol^{−1}).⁴⁴ The polymorphic phase transformation between EA·DNBA cocrystal is consistent with Ostwald's Rule of Stages,⁴⁵ which states that crystallization from solutions often starts in such a way that thermodynamically unstable phases appear first followed by recrystallization to thermodynamically stable phases. Unfortunately, the highly unstable nature of form II at RT prevented the application of other characterization method such as DSC and VT-PXRD to determine monotropic/enantiotropic relation between these polymorphs. Nevertheless, DSC analysis was performed on form I and the melting point was found to be 148.7 °C (Figure 4).

Neat grinding (NG) and SDG on a 1:1 molar ratio of EA and DNBA produced the stable form I without any contamination of form II. Figure 5 shows the comparison of some selected PXRD patterns of the samples obtained in the grinding experiments with varying solvent polarity. Attempts to obtain form II by varying the grinding time were not successful. After 5 min of NG, the PXRD pattern of the resulting powder revealed a physical mixture of EA and DNBA. Increasing the grinding time to 25 min even produced a physical mixture. However, NG for 30 min resulted in the stable form I. In contrast to the NG, SDG produced the stable form I even after 5 min of grinding (Figure S1, Supporting Information). All these observations suggest that the solid-state grinding techniques produce only the stable form I. However, we also postulate that because of its metastable nature even if form II was formed in the grinding experiments, it could convert into the most stable form I,

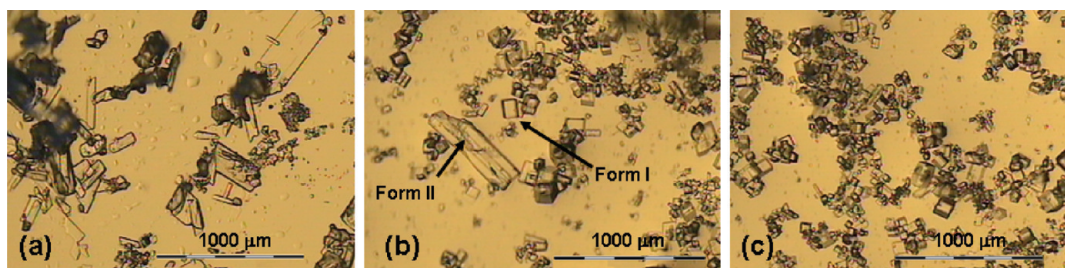


Figure 3. Snapshots of the nucleation and growth of form I & II at different time intervals: (a) after 10 min, (b) after 40 min, and (c) after 1 h.

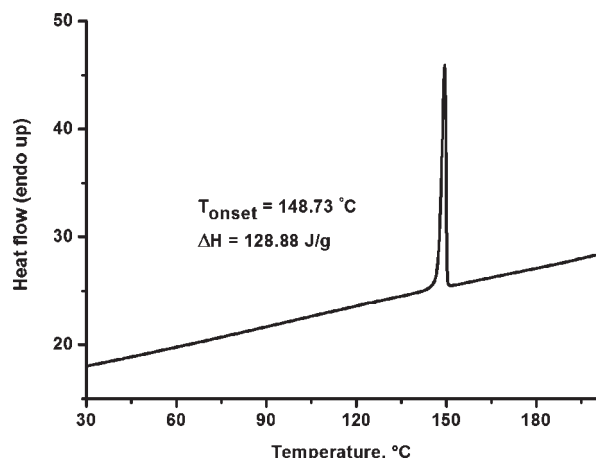


Figure 4. DSC trace of form I of the EA·DNBA cocrystal.

between the window period of running the grinding experiment and the running of PXRD experiment.

Synthon polymorphs are polymorphic crystal structures which differ by their different hydrogen bond synthons.^{46,47} This means that they exhibit different supramolecular synthons in different polymorphs. The analysis of polymorphic crystal structures as synthon polymorphs helps to understand the relative stabilities of the polymorphs based on intermolecular interactions that stabilize the solid-state structures. Synthon polymorphism has been realized recently in the cocrystal polymorphs.^{24–26} The polymorphs of EA·DNBA cocrystal can be best described as synthon polymorphs. Form I is sustained by an acid–amide heterosynthon, whereas form II is sustained by an amide–amide homosynthon (Figures 1 and 2). Nangia et al. evaluated the synthon energies of acid–amide heterosynthon vs their constituent homosynthons and found that acid–amide heterosynthon is energetically favorable compared to their constituent homosynthons.⁴⁸ This was further validated by the CSD analysis that the acid–amide heterosynthon is the most probable synthon when the acid and amide groups are present in a crystal structure.⁴⁹ The stability of form I of the EA·DNBA cocrystal can be judged by hydrogen bond preferences of the interacting amide and acid functionalities to form the acid–amide heterosynthon. In addition, form I is composed of zigzag chains of dimeric units held together by N–H···O hydrogen bonds. Crystal structure is further stabilized by various C–H···O and $\pi\cdots\pi$ stacking interactions. In contrast, form II consists of tetrameric motifs consisting of amide–amide homosynthons and such motifs are interconnected only by C–H···O and $\pi\cdots\pi$ stacking interactions. The stability of form I over form II was further confirmed by lattice energy calculations, which suggest that form I is more stable than form II by 6.1 kcal mol^{−1}.

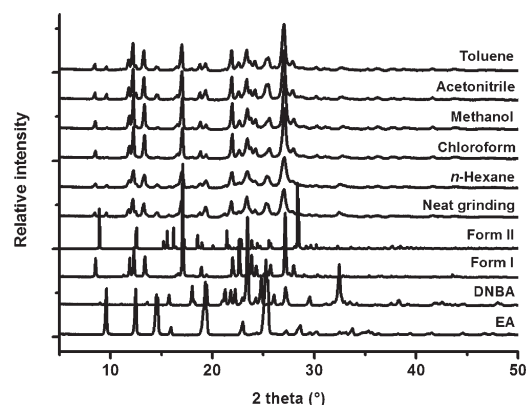


Figure 5. Comparison of PXRD patterns of the samples obtained in the grinding experiments on 1:1 EA and DNBA. The solvent used for the SDG is indicated on the right. The resulting powder materials contain a small amount of pure EA.

Solvates. In an attempt to prepare form II of the EA·DNBA cocrystal, EA and DNBA were crystallized in 1:1 molar ratio from a wide variety of organic solvents, such as methanol, ethanol, 2-propanol, acetone, 1,4-dioxane, tetrahydrofuran (THF), DCM, chloroform, dimethylsulfoxide, dimethylformamide, mesitylene, toluene, acetonitrile, ethyl acetate, *p*-xylene, and mixtures of one or more solvents. The crystallization experiments resulted either in the stable form I cocrystal or solvates. The cocrystal readily forms solvates with the following solvents: acetone, 1,4-dioxane, tetrahydrofuran (THF), mesitylene, toluene, acetonitrile, ethyl acetate, and *p*-xylene. All the solvates were characterized by ¹H NMR (see Figures S2–S9 in the Supporting Information), DSC, TGA and single crystal X-ray diffraction. For some of the solvated crystal structures (toluene, acetonitrile, ethyl acetate, and *p*-xylene solvates), the electron density is diffused for the guest portion and we could not obtain a better model for these disordered solvent molecules. Hence, the disordered solvent molecules were incorporated in the model using PLATON/SQUEEZE program.⁴³ In addition to the structural and thermochemical analysis, desolvation experiments were conducted to find out which of the two polymorphs of EA·DNBA cocrystal would result after desolvation.

Except for mesitylene solvate, all other solvates are isostructural with $P\bar{1}$ space group. Whereas acetonitrile has 1:1 host:guest stoichiometry, all other isostructural solvates possess 1:0.5 host:guest stoichiometry. In all these cases, guest molecules sit on a general position and they are disordered over two positions with a 50% site occupancy factor, except for the 1,4-dioxane which is fully ordered.

The crystal structures of the isostructural solvates of EA·DNBA cocrystal bear close resemblance to the crystal

structure of form II of EA·DNBA cocrystal. Similar to form II of EA·DNBA cocrystal (Figure 2), in the EA·DNBA solvates, the two inversion-related EA molecules are sustained by amide–amide homosynthon and these molecules form tetrameric motifs with two DNBA molecules. These tetrameric motifs stack along the crystallographic *a*-axis and generate rectangular voids in the *bc* plane for guest inclusion (Figure 6).

In the acetone solvate, EA·DNBA·0.5(C₃H₆O), the tetrameric motif is the basic structural unit. The disordered acetone molecule is surrounded by two molecules each of EA and DNBA and stabilized by C–H···O interactions (2.58 Å, 125°; 2.42 Å, 164°) from the aromatic C–H groups of the EA and DNBA molecules to the C=O group of the disordered acetone (Figure 7a). The void size, which was

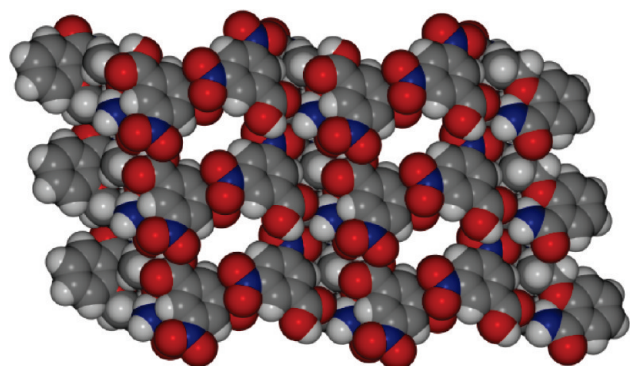


Figure 6. Packing diagram (space filling model) of the crystal structure of EA·DNBA·1,4-dioxane showing the voids for guest inclusion. The guest molecules in the voids are not shown here.

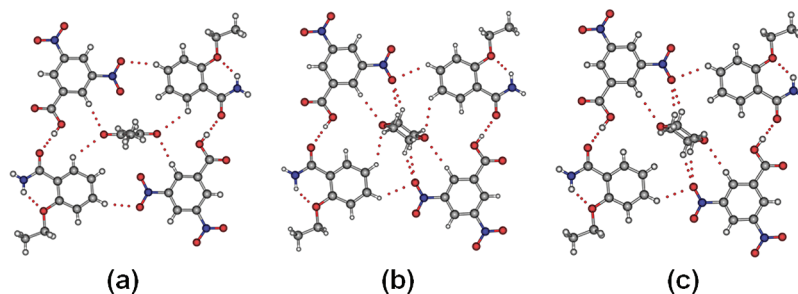


Figure 7. Packing diagram of (a) acetone, (b) 1,4-dioxane, and (c) THF solvates of EA·DNBA cocrystal to show host–guest interactions. Notice that THF mimics the 1,4-dioxane molecule.

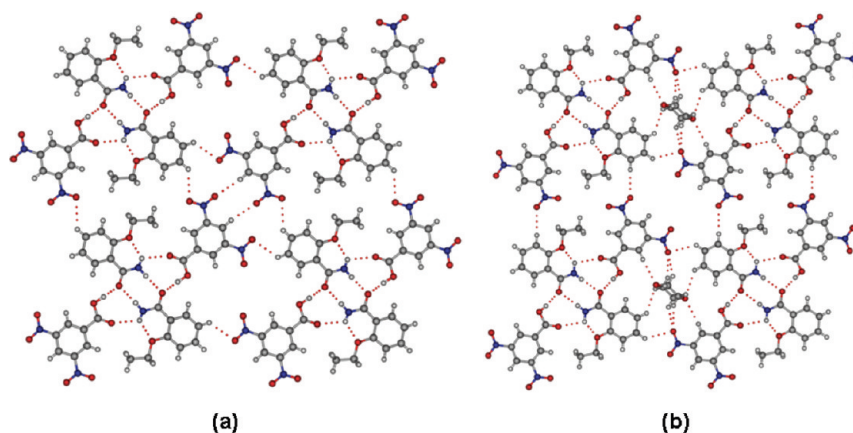


Figure 8. Comparison of packing diagrams of (a) form II and (b) 1,4-dioxane solvate of the EA·DNBA cocrystal. Notice the absence of C–H···O interactions between the DNBA molecules in the solvated structure.

calculated by measuring the centroid–centroid distance of all four surrounding host molecules, is $8.1 \times 8.2 \text{ \AA}^2$.

The packing of the 1,4-dioxane solvate, EA·DNBA·0.5-(C₄H₈O₂) and THF solvate EA·DNBA·0.5(C₄H₈O), is isostructural to that of the acetone solvate with the tetrameric motif being the basic structural unit and guest molecule surrounded by two molecules each of EA and DNBA. While the 1,4-dioxane molecule is fully ordered, THF molecule is disordered and mimics 1,4-dioxane. In both cases, the guest molecule is stabilized in the host cavity by several host···guest and guest···host C–H···O (2.44–2.64 Å, 127–160°) interactions (Figure 7b,c). Despite having a bigger guest (1,4-dioxane and THF), there was no significant increase in the size of the rectangular voids when compared to the acetone solvate ($8.1 \times 8.3 \text{ \AA}^2$ in 1,4-dioxane solvate vs $8.1 \times 8.2 \text{ \AA}^2$ in acetone solvate).

The isostructural solvates and form II of the EA·DNBA cocrystal contain the same basic structural motif (tetrameric motif). The self-assembly of the tetrameric motifs in the form II and 1,4-dioxane solvate is compared in Figure 8. There are no significant differences in the hydrogen bond metrics that build the tetrameric motifs (see Table S2 in the Supporting Information). As can be easily recognized, two C–H···O (2.45 Å, 172°) interactions between the DNBA molecules are the key intermolecular interactions that hold the tetrameric motifs in form II, in addition to the C–H···O interactions between EA and DNBA molecules. The inclusion of guest molecule (1,4-dioxane) forces host molecules in these motifs to move farther away from each other in the solvated structures. Consequently, the C–H···O interactions between the two DNBA molecules are absent in the solvated structure. In addition, the interlayer distance between the

two tetrameric motifs is longer than that of the interlayer distance in form II (3.39 Å vs 3.32 Å). It should be noted that the supramolecular interactions that hold the tetrameric motifs in both of these crystal structures are C–H···O interactions, however, form II has a greater number of these interactions.

Crystal packing in the other solvates (toluene, acetonitrile, ethyl acetate, and *p*-xylene) of the EA·DNBA cocrystal is similar to the solvates described above, consisting of tetrameric motif mediated by an amide–amide homosynthon and channels along the crystallographic *a*-axis where guest molecules are located. The details of host–host interactions were provided in the Table S2 in the Supporting Information.

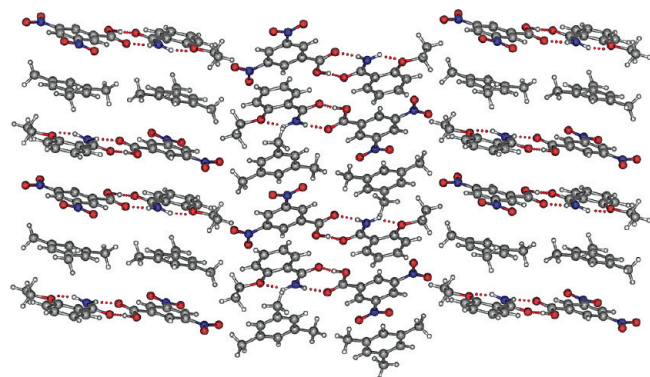


Figure 9. Packing diagram showing the stacking interactions in the crystal structure of mesitylene solvate of EA·DNBA cocrystal.

Cocrystallization of EA and DNBA from mesitylene afforded a solvate, EA·DNBA·(C₉H₁₂), in monoclinic, *P*2₁/*c* space group. The mesitylene molecule is fully ordered. Interestingly, EA and DNBA molecules are now engaged in the formation of an acid–amide heterosynthon involving N–H···O (1.93 Å, 168°) and O–H···O (1.55 Å, 171°) hydrogen bonds. Unlike the other solvated structures, voids are absent in this structure and the mesitylene molecules are sandwiched between two dimeric motifs (Figure 9). The overall crystal structure is stabilized by infinite aromatic π···π interactions.

Figure 10 shows the results of the TGA and DSC experiments on the acetone, 1,4-dioxane, THF, and mesitylene solvates of EA·DNBA cocrystal. TGA analysis confirms the host:guest stoichiometry obtained from the X-ray (Table 1) and ¹H NMR analysis. Based on the TGA and DSC curves it can be judged that the desolvation occurs in a single step. All the solvates show a broad endotherm for the desolvation which is consistent with the weight loss step in the TGA curves. The second endotherm in the DSC analysis corresponds to the melting point of the remaining solid after the desolvation. The 1,4-dioxane solvate shows a small exotherm after the guest release which is ascribed to the crystallization of a small amount of the desolvated material before the melting. The solids obtained after removal of the solvent belong to cocrystal form I and melt within a temperature range of 148 ± 1 °C depending on the solvent included in the crystal lattice. This was further confirmed by desolvation experiments performed separately on the crystalline solvates (discussed next). The *T*_{on} values for the guest release match with the boiling point of the solvent for acetone, 1,4-dioxane,

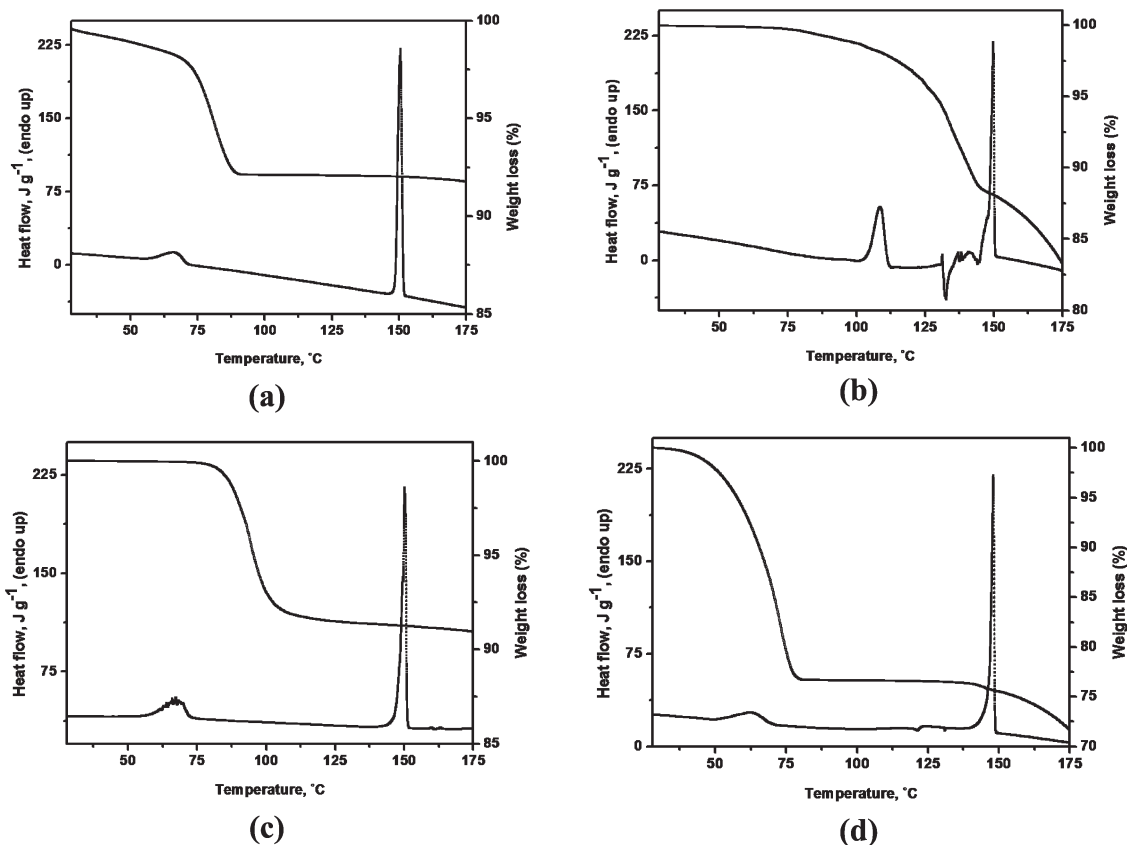


Figure 10. DSC and TGA traces of EA·DNBA cocrystal solvates: (a) acetone, (b) 1,4-dioxane, (c) THF, and (d) mesitylene. DSC/TGA traces for other solvates were provided in the Supporting Information (Figure S10).

Table 1. Thermal Data (DSC and TGA) for EA·DNBA Cocrystal Solvates

guest molecule	calcd weight loss (%)	obsd weight loss in TGA (%)	guest loss T_{on} in DSC (°C)	ΔH for guest loss (J g ⁻¹)	solvent boiling point (°C)
acetone	6.67	7.73	56.96	27.89	57
1,4-dioxane	9.47	^a	104.72	40.66	101
thf	8.02	8.45	66.83	37.54	66
mesitylene	24.16	23.80	56.13	26.11	165
toluene	9.81	11.57	79.90	39.52	111
acetonitrile	9.81	9.61	55	29.46	82
ethylacetate	9.46	8.80	75.63	31.44	77
<i>p</i> -xylene	10.98	12.73	89.17	20.06	138

^aTGA did not show a clear step for desolvation.

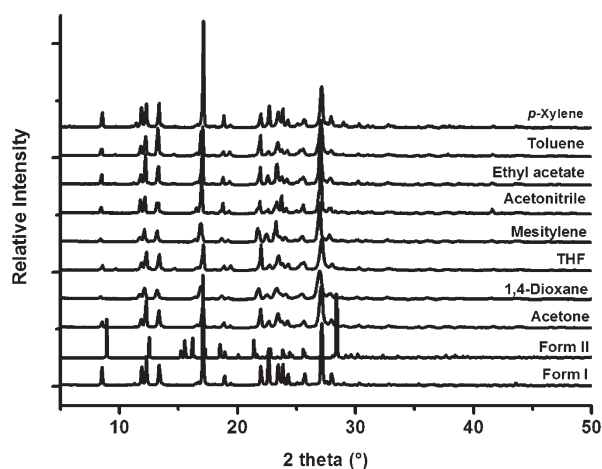


Figure 11. Comparison of PXRD patterns of the samples obtained in the desolvation experiments on the solvates of EA·DNBA cocrystal. The solvent present in a particular solvate is indicated on the right. Notice that all the patterns match with form I of the EA·DNBA cocrystal.

THF, and ethylacetate. The T_{on} values for the release of the acetonitrile, and aromatic hydrocarbon guests (mesitylene, toluene, and *p*-xylene) are much lower than their respective boiling point. This could be because of the absence of strong hydrogen bonds between the host cavity and the guest molecule.

Desolvation experiments on the solvated crystals were conducted to identify which of the two polymorphs of the EA·DNBA cocrystal would result after desolvation. Crystals obtained from the crystallization experiments were heated on a hot plate for an hour at 100 °C. The desolvation can be easily realized by the loss of solvent from the crystals, which was judged by complete opaqueness of the crystals. Interestingly, the outward shape of the crystals was unchanged even after complete desolvation. Desolvation of all of the solvates yielded the cocrystal form I. This was demonstrated by recording the PXRD traces of the desolvated materials and finding that they correspond with the experimental PXRD pattern of form I (Figure 11).

Structural rearrangement with concomitant loss of crystallinity is usually observed upon desolvation under reduced pressure or by thermal treatment.⁵⁰ In the case of cocrystal solvates, there are several possible outcomes of desolvation: for example, (i) the cocrystal may dissociate into its components and exist as a physical mixture, (ii) the remaining crystal lattice may remain essentially unchanged compared to the solvate as in the case of zeolites, (iii) the desolvation may result in a physical mixture containing partially crystalline or amorphous materials of cocrystal components, and

Table 2. CSD Statistics on the Prevalence of Polymorphism and Hydrate/Solvate Formation in Single Component vs Cocrystals.^a

	no. of entries	%
cocrystals	3624	100 ^b
polymorphic cocrystals	44	1.2
cocrystal hydrates	451	12.4
cocrystal solvates	394	10.9
organic structures excluding cocrystals	135997	100 ^b
single-component polymorphs	2035	1.5
hydrates	6835	5.0
solvates	12539	9.2

^aThe CSD Conquest May 2009 release contains a total of 156 196 nonionic organic crystal structures for which 3D coordinates were determined. Structures containing two or more solids were considered as cocrystals. ^bPercentages were calculated separately based on 135 997 and 3624 subtotals, respectively.

(iv) the desolvated form may have a lattice structure that is different from the original material. Because of the fragile nature of organic solids¹⁷ which are held together by intermolecular interactions, removal of the guest molecules would likely induce complete collapse of the structure. Thus, we anticipate that first of the four possibilities mentioned above could be the most probable outcome in the desolvation of a cocrystal solvate. In the case of EA·DNBA cocrystal solvates, surprisingly, the desolvation produced form I at the expense of form II which contains a similar hydrogen bonding motif with the solvate structures. It is worth to highlight that the transformation from the solvated structure to form I involves a switch over of the supramolecular synthon from an amide–amide homosynthon (solvate) to an acid–amide heterosynthon (form I). Furthermore, it can be envisaged that the formation of form I in the desolvation proceeds through form II because of its structural similarity with the isostructural solvates. As shown in Figure 8, upon removal of the solvent molecules which are located between the tetrameric motifs, there is only a minimal structural rearrangement required to convert into form II. However, the metastable nature of form II might have prevented it from being obtained as the final desolvation product. Even if solvates have converted to form II immediately upon the loss of solvent, form II would readily transform to the stable form I and thus form I was observed instead.

CSD Analysis on Cocrystal Polymorphs and Solvates. With our interest in cocrystal polymorphs and solvates, we sought to find out the tendency of cocrystals to form polymorphs and solvates by analyzing the cocrystals deposited in the CSD. There are a total of 3624 cocrystals present in the CSD (Table 2), of which 44 cocrystals are polymorphic (see the Supporting Information for a full list of all the polymorphic cocrystals, Table S3). Including two recently reported cocrystal polymorphs of EA, a total of 46 polymorphic cocrystals

were reported to date. Of these 46 cocrystals, 33 cocrystals are sustained by strong hydrogen bonding and the remaining 13 cocrystals are sustained only by weak interactions. Crystal structures of all the polymorphic cocrystals were further analyzed manually to recognize the structure stabilizing interactions in terms of supramolecular synthons anticipating that such analysis would provide possible reasons for the polymorphism in cocrystals. Interestingly, in most of the cocrystal polymorphs (in 41 polymorphs, 89%), the primary supramolecular synthon that holds the cocrystal components are persistent and it appears that small conformational differences and various other factors such as contribution from other structure stabilizing interactions play an important role. The remaining 5 cocrystals (11%) can be classified as synthon polymorphs. Of these, 3 are stabilized by strong hydrogen bonds (CSD refcodes: ODOBIT, UNEZAO, and WOBQEK) and the remaining 2 are stabilized by weak interactions (CSD refcodes: NARSOP and SEOTCR). In the case of EA cocrystals, 2 of the 3 polymorphic cocrystals (EA·saccharin²⁰ and EA·gentisic acid²¹) retain the supramolecular synthons in their respective polymorphic structures and in all of the polymorphs at least one of the constituent molecules adopts a slightly different conformation. Comparison of the CSD statistics on the polymorphic single component crystals with that of the polymorphic cocrystals (Table 2) reveals that approximately an equal percentage of cocrystals exhibit polymorphism. Interestingly, the number of cocrystal polymorphs that were reported after the year 2000 is double the number of cocrystal polymorphs reported before (32 vs 14, Table S3 in the Supporting Information). We believe this is due to the surge of research activity toward the development of cocrystal materials as cocrystals are showing potential relevance in the fields of pharmaceuticals,^{1–14} electronic and optical materials,⁵¹ semiconductors,⁵² and solid-state organic synthesis.⁵³ This has led to cocrystal research in more diverse directions, including exhaustive screening, process development and scale up as well as stability investigations. As a result of increasing efforts devoted toward polymorph screening of cocrystal, the number of reported cocrystal polymorphs has increased over time. In this respect, it can be reasonable to speculate that the famous McCrone's statement that "the number of polymorphic forms known for a given compound is proportional to the time and money spent in research on that compound"⁵⁴ may be applicable even to multicomponent crystals such as cocrystals.

CSD analyses have also been carried out recently to retrieve the solvates/hydrates.^{55–64} While Streek provided a list of all series of solvates (including hydrates) and their unsolvated forms,⁵⁵ Desiraju analyzed crystalline hydrates,⁵⁶ and Brychczynska et al. studied the role of incorporated methanol in the crystal lattice.⁵⁷ Infantes et al. analyzed the water clusters in terms of hydrogen-bonded motifs and also examined the various factors that influence the hydration in organic crystals.^{62–64} However, none of these studies focused exclusively on the cocrystal solvates/hydrates,⁶⁵ which prompted us to carry out such a study to examine the likelihood of cocrystal to form solvates/hydrates. The results of the CSD search were tabulated in Table 2. Of the 3624 cocrystals deposited in the CSD, 451 (12.4%) structures were identified with water molecules and a majority (88%) of these 451 structures contain only water (pure hydrates). The remaining 12% of the 451 structures contain one or more of the other solvents together with water

Table 3. Ten Most Commonly Observed Solvents in Cocrystal Solvates

rank	solvent	occurrences	ordered structures	% of occurrence ^a
1	toluene	55	7	13.9
2	methanol	45	31	11.4
3	acetonitrile	38	25	9.6
4	ethanol	37	17	9.4
5	chloroform	34	15	8.6
6	DCM	33	17	8.4
7	benzene	31	24	7.9
8	acetone	11	4	2.8
9	dimethylsulfoxide	11	5	2.8
10	ethyl acetate	10	8	2.5

^aPercentage with respect to the 394 cocrystal solvates.

molecules. Methanol, ethanol, and acetonitrile were found to be the top three solvents that are incorporated together with water in the cocrystals. This could be because of the fact that these solvents are completely miscible with water and also possess strong hydrogen-bond donors/acceptors. Solvates were accounted for 10.9% (394) of the total cocrystals. A search to retrieve the crystal structures in which there is only one solid component resulted in 6835 (5.0%) hydrates⁶⁶ and 12539 (9.2%) solvates. Comparison of these statistics with cocrystal hydrates/solvates suggests that the cocrystals have greater ability to form solvates/hydrates. Intriguingly, whereas the percentage of cocrystals forming hydrates and solvates is approximately equal (12.4 vs 10.9%); the percentage of solvated structures in which there is only one solid component is almost double when compared to the hydrated structures (9.2 vs 5.0%). In addition, the percentage of hydrates is more than 2 times greater for cocrystals (12.4 vs 5.0%). These statistics clearly demonstrate the greater affinity of cocrystals to form solvates/hydrates among the structures deposited in the CSD.

In a database study performed a decade ago, Nangia and Desiraju found that about 15% of organic crystals are solvated; furthermore dimethylformamide, Dimethylsulfoxide and 1,4-dioxane were found to be most commonly incorporated solvents in the crystals.⁵⁸ The high probability of occurrence of these solvents was rationalized by their ability to participate in multipoint recognition via either strong (O/N–H···O) or weak (C–H···O) hydrogen bonds. A subsequent database analysis by Görbitz and Hersleth validated these statistics and reported the frequency of occurrences of 50 common organic solvents in the crystal lattices.⁵⁹ On the basis of their search criteria, it was found that methanol, DCM, and benzene are the top three solvents that are most commonly observed in the crystal structures. The prevalence of these solvents could also indicate the chemist's preference to use these solvents in the synthesis and crystallization experiments. The cocrystal solvates that were retrieved in the present database analysis were further analyzed to estimate the frequency of occurrence of the incorporated solvent molecules. Table 3 shows the top 10 most commonly observed solvents with their frequency of occurrence given in percentage. Toluene, methanol, and acetonitrile are the top three solvents with frequency of occurrence of 13.9, 11.4, and 9.6%, respectively. However, it was observed that more than half of these crystal structures (202 of the 394 solvates) contain disordered solvent molecules. Toluene molecule is found to be disordered in most (48 of 55) of the cocrystal solvates. Among the fully ordered solvent molecules, methanol, acetonitrile and benzene are most commonly observed in the cocrystal solvates with

number of occurrences of 31, 25, and 24, respectively. An in-depth analysis of all the cocrystal hydrate/solvate structures in terms of their structure stabilizing interactions could shed further light on the greater affinity of cocrystals to form hydrates/solvates, but this will be out of the main focus of this paper which is to explore the form diversity of EA·DNBA cocrystal. However, we surmise that the solvate formation in cocrystals could be partly due to the formation of open structures attributable to inefficient packing of hydrogen-bonded aggregates in the cocrystals. The EA·DNBA cocrystal represents a remarkable example to support this statement. The hydrogen-bonded aggregate in the unstable polymorph (tetrameric motif in form II) is stabilized in the solvates by the inclusion of solvent molecules. On the basis of the analysis of all organic hydrates deposited in the CSD, it has been recently found that the ratio of hydrogen bond donor/acceptor groups does not have any significant effect on the frequency of hydrate formation.⁶⁴ Whether or not this is true in the case of cocrystal hydrates/solvates can be validated only by a detailed analysis of all these structures.

Conclusions

Despite its simple molecular structure, the structural chemistry of EA in its cocrystals is remarkable in the sense that three of its cocrystals are polymorphic (including the polymorphs of EA·saccharin and EA·gentisic acid cocrystals), and one of them (EA·DNBA cocrystal) also forms multiple solvates. The cocrystal studied herein demonstrates the interplay of supramolecular synthons in stabilizing the cocrystal polymorphs and solvates. The polymorphs of the EA·DNBA cocrystal can be best described as synthon polymorphs. It is interesting that all of the solvates described here revert to the stable polymorph (form I) upon desolvation. The desolvation experiments help to demonstrate the switch over of the supramolecular synthon to form the stable polymorph. Thermochemical measurements have established the stability of polymorphs and solvates. Analysis of the cocrystals deposited into the CSD suggests that the number of cocrystal polymorphs being added to the database is increasing in recent years. We believe that this could be because of the overwhelming interest in the development of pharmaceutical cocrystals. It was also found that the percentage of crystal structures that are hydrates/solvates is much higher for cocrystals when compared to the crystalline hydrates/solvates of a solid component, and we believe that this warrants further in-depth analysis to unveil the factors that are responsible for this tendency. The CSD statistics strongly support the results obtained so far on various EA cocrystals.

Acknowledgment. This work was supported by the Institute of Chemical and Engineering Sciences of A*STAR (Agency for Science, Technology and Research), Singapore.

Supporting Information Available: X-ray crystallographic information files (CIF); tables listing key crystallographic parameters and hydrogen-bond distances, PXRD patterns of the samples obtained in the grinding experiments with varying grinding time, ¹H NMR analysis of the solvates, a list of polymorphic cocrystals, and a list of refcodes obtained in the CSD analysis (PDF). This material is available free of charge via the Internet at <http://pubs.acs.org>.

References

- (1) Vishweshwar, P.; McMahon, J. A.; Zaworotko, M. J. In *Frontiers in Crystal Engineering* Tiekink, E. R. T., Vittal, J. J., Eds.; Wiley: Chichester, U.K., 2006; pp 25–49.
- (2) Remenar, J. F.; Morissette, S. L.; Peterson, M. L.; Moulton, B.; MacPhee, J. M.; Guzman, H. R.; Almarsson, Ö. *J. Am. Chem. Soc.* **2003**, *125*, 8456.
- (3) McNamara, D. P.; Childs, S. L.; Giordano, J.; Iarricchio, A.; Cassidy, J.; Shet, M. S.; Mannion, R.; O'Donnell, E.; Park, A. *Pharm. Res.* **2006**, *23*, 1888.
- (4) Hickey, M. B.; Peterson, M. L.; Scoppettuolo, L. A.; Morissette, S. L.; Vetter, A.; Guzmán, H.; Remenar, J. F.; Zhang, Z.; Tawa, M. D.; Haley, S.; Zaworotko, M. J.; Almarsson, Ö. *Eur. J. Pharm. Biopharm.* **2007**, *67*, 112.
- (5) Updated list of GRAS chemicals may be downloaded from <http://www.cfsan.fda.gov/~dms/efafus.html>.
- (6) Almarsson, Ö.; Zaworotko, M. J. *Chem. Commun.* **2004**, 1889.
- (7) Trask, A. V. *Mol. Pharm.* **2007**, *4*, 301.
- (8) Schultheiss, N.; Newman, A. *Cryst. Growth Des.* **2009**, *9*, 2950.
- (9) Stahly, G. P. *Cryst. Growth Des.* **2009**, *9*, 4212.
- (10) Good, D. J.; Rodríguez-Hornedo, N. *Cryst. Growth Des.* **2009**, *9*, 2252.
- (11) Bak, A.; Gore, A.; Yanez, E.; Stanton, M.; Tufekcic, S.; Syed, R.; Akrami, A.; Rose, M.; Surapaneni, S.; Bostick, T.; King, A.; Neervannan, S.; Ostovic, D.; Koparkar, A. *J. Pharm. Sci.* **2008**, *97*, 3942.
- (12) Trask, A. V.; Sam Motherwell, W. D.; Jones, W. *Int. J. Pharm.* **2006**, *320*, 114.
- (13) Basavoju, S.; Boström, D.; Velaga, S. P. *Cryst. Growth Des.* **2006**, *6*, 2699.
- (14) Trask, A. V.; Motherwell, W. D. S.; Jones, W. *Cryst. Growth Des.* **2005**, *5*, 1013.
- (15) Bernstein, J. *Polymorphism in Molecular Crystals*; Clarendon: Oxford, U.K., 2002.
- (16) MacNicol, D. D.; Toda, F.; Bishop, R. *Solid-State Supramolecular Chemistry, Crystal Engineering*; Comprehensive Supramolecular Chemistry; Pergamon Press: Oxford, U.K., 1996; Vol. 6.
- (17) Nassimbeni, L. R. *Acc. Chem. Res.* **2003**, *36*, 631.
- (18) Nangia, A. In *Nanoporous Materials: Science and Engineering*; Lu, G. Q., Zhao, X. S., Eds.; Imperial College Press: London, 2004; pp 165–187.
- (19) Byrn, S. R.; Pfeiffer, R. R.; Stowell, J. G. *Solid-State Chemistry of Drugs*, 2nd ed.; SSCI Inc.: West Lafayette, IN, 1999.
- (20) Aitipamula, S.; Chow, P. S.; Tan, R. B. H. *CrystEngComm* **2009**, *11*, 889.
- (21) Aitipamula, S.; Chow, P. S.; Tan, R. B. H. *CrystEngComm* **2009**, *11*, 1823.
- (22) Braga, D.; Palladino, G.; Polito, M.; Rubini, K.; Grepioni, R.; Chierotti, M. R.; Gobetto, R. *Chem.—Eur. J.* **2008**, *14*, 10149.
- (23) Sokolov, A. N.; Swenson, D. C.; MacGillivray, L. R. *Proc. Natl. Acad. Sci.* **2008**, *105*, 1794.
- (24) Babu, N. J.; Reddy, L. S.; Aitipamula, S.; Nangia, A. *Chem. Asian J.* **2008**, *3*, 1122.
- (25) Porter, W. W., III.; Elie, S. C.; Matzger, A. J. *Cryst. Growth Des.* **2008**, *8*, 14.
- (26) Sreekanth, B. R.; Vishweshwar, P.; Vyas, P. *Chem. Commun.* **2007**, 2375 and references therein.
- (27) ter Horst, J. H.; Cains, P. W. *Cryst. Growth Des.* **2008**, *8*, 2537.
- (28) Vishweshwar, P.; McMahon, J. A.; Peterson, M. L.; Hickey, M. B.; Shattock, T. R.; Zaworotko, M. J. *Chem. Commun.* **2005**, 4601.
- (29) Friščić, T.; Trask, A. V.; Motherwell, W. D. S.; Jones, W. *Cryst. Growth Des.* **2008**, *8*, 1605.
- (30) Banerjee, R.; Bhatt, P. M.; Desiraju, G. R. *Cryst. Growth Des.* **2006**, *6*, 1468.
- (31) Bhogala, B. R.; Basavoju, S.; Nangia, A. *Cryst. Growth Des.* **2005**, *5*, 1683.
- (32) Thallapally, P. K.; Dobrzańska, L.; Gingrich, T. R.; Wirsig, T. B.; Barbour, L. J.; Atwood, J. L. *Angew. Chem., Int. Ed.* **2006**, *45*, 6506.
- (33) Atwood, J. L.; Barbour, L. J.; Jerga, A.; Schottel, B. L. *Science* **2002**, *298*, 1000.
- (34) Karki, S.; Friščić, T.; Jones, W.; Motherwell, W. D. S. *Mol. Pharm.* **2007**, *4*, 347.
- (35) Uehara, H.; Otsuka, K.; Izumi *Cancer Letters* **1998**, *135*, 83.
- (36) Aoki, S.; Mizutani, T.; Danjo, D. *Chem. Pharm. Bull.* **2000**, *48*, 140.
- (37) Kawano, O.; Sawabe, T.; Misaki, N.; Fukawa, K. *Jpn. J. Pharmacol.* **1978**, *28*, 829.
- (38) Moribe, K.; Tsuchiya, M.; Tozuka, Y.; Yamaguchi, K.; Oguchi, T.; Yamamoto, K. *Chem. Pharm. Bull.* **2004**, *52*, 524.
- (39) Pagola, S.; Stephens, P. W. *Acta Crystallogr., Sect. C* **2009**, *65*, o583.
- (40) *Cambridge Structural Database (version 5.29) ConQuest 1.10*, May 2009 update; Cambridge Crystallographic Data Centre, Cambridge, U.K., 2007; to be found under www.ccdc.cam.ac.uk.

- (41) Sheldrick, G. M. *SHELXS-97 and SHELXL-97, Programs for the Solution and Refinement of Crystal Structures*; University of Göttingen, Göttingen, Germany, 1997.
- (42) It should be mentioned here that the CSD does not contain information pertaining to pharmaceutical relevance of many co-crystal components, and it is often difficult to judge whether a particular compound is pharmaceutically relevant or not just based on its compound name. Hence, our estimation of pharmaceutical cocrystals is based on a general search of all these compounds, and it is possible that the actual number of pharmaceutical cocrystals could be more than 137 of the total 3624 cocrystals.
- (43) Spek, A. L. *Acta Crystallogr., Sect. D* **2009**, *65*, 148.
- (44) Computed in Materials Studio using Forcite module, COMPAS force field. www.accelrys.com.
- (45) Ostwald, W. Z. *Phys. Chem.* **1897**, *22*, 289.
- (46) Jetti, R. K. R.; Boese, R.; Sarma, J. A. R. P.; Reddy, L. S.; Vishweshwar, P.; Desiraju, G. R. *Angew. Chem., Int. Ed.* **2003**, *42*, 1963.
- (47) Nangia, A.; Desiraju, G. R. *Top. Curr. Chem.* **1998**, *198*, 57.
- (48) Vishweshwar, P.; Nangia, A.; Lynch, V. M. *Cryst. Growth Des.* **2003**, *3*, 783.
- (49) McMahon, J. A.; Bis, J. A.; Vishweshwar, P.; Shattock, T. R.; McLaughlin, O. L.; Zaworotko, M. J. Z. *Kristallogr.* **2005**, *220*, 340.
- (50) Caira, M. R.; Nassimbeni, L. R. *Comprehensive Supramolecular Chemistry*; Atwood, J. L., Davies, J. E. D., MacNicol, D., Vögtle, F., Eds.; Elsevier Science: Oxford, U.K., 1996; Vol. 6, pp 825–850.
- (51) Etter, M. C.; Frankenbach, G. M.; Adsmund, D. A. *Mol. Cryst. Liq. Cryst.* **1990**, *187*, 285.
- (52) Sokolov, A. N.; Friščić, T.; MacGillivray, L. R. *J. Am. Chem. Soc.* **2006**, *128*, 2806.
- (53) MacGillivray, L. R.; Papaefstathiou, G. S.; Friščić, T.; Hamilton, T. D.; Bučar, D. –K.; Chu, Q.; Varshney, D. B.; Georgiev, I. G. *Acc. Chem. Res.* **2008**, *41*, 280.
- (54) McCrone, W. C. In *Polymorphism in Physics and Chemistry of the Organic Solid State*; Fox, D., Labes, M. M., Weissberger, A., Eds.; Wiley Interscience: New York, 1965; Vol. 2, pp 725–767.
- (55) van de Streek, J. *CrystEngComm* **2007**, *9*, 350.
- (56) Desiraju, G. R. *J. Chem. Soc., Chem. Commun.* **1991**, 426.
- (57) Brychczynska, M.; Davey, R. J.; Pidcock, E. *New J. Chem.* **2008**, *32*, 1754.
- (58) Nangia, A.; Desiraju, G. R. *Chem. Commun.* **1999**, 605.
- (59) Görbitz, C. H.; Hersleth, H. –P. *Acta Crystallogr., Sect. B* **2000**, *56*, 526.
- (60) van de Streek, J.; Motherwell, S. *CrystEngComm* **2007**, *9*, 55.
- (61) Gillon, A. L.; Feeder, N.; Davey, R. J.; Storey, R. *Cryst. Growth Des.* **2003**, *3*, 663.
- (62) Infantes, L.; Motherwell, S. *CrystEngComm* **2002**, *4*, 454.
- (63) Infantes, L.; Chisholm, J.; Motherwell, S. *CrystEngComm* **2003**, *5*, 480.
- (64) Infantes, L.; Fábíán, L.; Motherwell, W. D. S. *CrystEngComm* **2007**, *9*, 65.
- (65) As part of an analysis of the occurrence of pharmaceutically acceptable anions and cations in the CSD, Haynes et al. retrieved the hydrates of cocrystals that contain at least one pharmaceutically acceptable acid or base. It was found that, of the 381 total cocrystals, 59 (15.5%) were hydrates. See Haynes, D. A.; Jones, W.; Motherwell, W. D. S. *J. Pharm. Sci.* **2005**, *94*, 2111.
- (66) It should be noted here that the search criteria that was followed in the current database analysis to retrieve the hydrates did not include the ionic structures and hence the statistics reported do not match with the statistics reported by Infantes et al. The reported statistics were based only on the cocrystals and single component crystal structures of the neutral molecules. It is well-known that the presence of charged groups, such as Ca^{2+} , COO^- , etc., significantly increases the chances of forming hydrates (see refs 63 and 65).